Progress In Electromagnetics Research M, Vol. 80, 133–143, 2019

Energy-Efficient Coding Matrix FMD-RDA Secure Transmission Scheme Based on Quadrature Spatial Modulation for mmWave Systems

Shaddrack Y. Nusenu[1, 2, *] **and Abdul Basit**[1, 3]

Abstract—Artificial noise (AN) aided method in mmWave is hard to realize due to large transmit antennas and also requires additional power. This paper proposes coding matrix secure transmission based on quadrature spatial modulation (QSM) utilizing a frequency modulated diverse retrospective array (FMD-RDA). Specifically, we adopt coding matrix for frequency increment with QSM symbols to form part of FMD-RDA angular-range array factor. Consequently, low probability of detection (LPD) is created during the QSM transmission without additional power. The desired receiver should know the particular coding matrix a priori. Importantly, the system has automatic user tracking ability with no channel state information (CSI) needed at the desired receiver and can handle receivers with highly correlated channels. Further, secrecy outage probability (SOP), asymptotic lower bound on eavesdropper's (Eve's) detecting error probability and average data leakage rate are analyzed without Eve's CSI. Simulation results show that increasing the coding matrix, satisfactory secrecy is attained for the proposed scheme. Moreover, through the results certain essential secrecy information has been highlighted that is not captured by the classical SOP making the proposed scheme an attractive technique for QSM applications.

1. INTRODUCTION

Millimeter wave (mmWave) system has been one of the attractive systems to meet the data capacity especially for fifth-generation (5G) wireless technology [1] and even beyond. The mmWave provides abundant bandwidth spectrum, rangeing from 30 GHz (with wavelength 10 mm) to 300 GHz (with wavelength 1 mm), which can be explored to significantly increase the data rate. Additionally, mmWave offers small wavelength that makes it possible for large antennas to be deployed in a small physical area [2–4]. In the literature, several authors have investigated smart antennas which are also feasible in mmWave communication applications [5–14].

In recent years, spatial modulation (SM) technique [15, 16] as an alternative multi-antenna scheme has attracted much attention. The SM scheme has many promising advantages and is primarily focused on communication applications to provide spectral efficiency, low complexity design, and reliability [17–20]. Due to the massive connectivities of users in 5G mmWave technology as a result of the broadcast nature of wireless characteristics, it is important to tackle security issues.

Physical layer security (PLS) has been investigated [21, 22] which is proven to improve the wireless systems secrecy [23–25]. Several authors have investigated SM based PLS techniques [26–31]. Very recently, a new variant of SM, namely quadrature spatial modulation (QSM), was proposed [32] to alleviate the drawbacks of SM [15, 16].

Received 14 February 2019, Accepted 28 March 2019, Scheduled 11 April 2019

[*] Corresponding author: Shaddrack Y. Nusenu (nusenu2012gh@yahoo.com).

[1] University of Electronic Science and Technology of China (UESTC), China. [2] Koforidua Technical University (KTU), Ghana. [3] International Islamic University, Islamabad, Pakistan.

In [33], AN security method was developed for QSM scheme. Although AN methods offer security, in mmWave more transmit antennas can be deployed due to small wavelength, hence, AN implementation will be difficult to realize practically [34]. Secondly, AN causes the data transmission power to decrease leading to reduction of signal-to-interference-plus noise ratio at the desired receiver. Thirdly, in channels that are highly correlated, AN failed to provide better security [35]. Therefore, alternative security methods with low energy consumption have to be considered.

In recent years, retrodirective array (RDA) [36] which can offer self-tracking automatically and facilitate retransmission of signal along interrogator direction with no priori knowledge of the arrival of the incoming angle has been investigated in [37–39]. More importantly, utilizing RDA does not required CSI (i.e., bandwidth can be saved) at the receiver. Note that in most of the existing QSM systems require CSI at the receiver for retrieving the information bits [40–42].

In this paper, we propose secure transmission based on QSM utilizing FMD-RDA for mmWave systems. Explicitly, coding matrix is adopted to design the small frequency increment and embed the QSM bits as part of the FMD-RDA range-angle array factor. Consequently, we can create low probability of detection (LPD) during the QSM transmission without additional power. It is assumed that the desired receiver knows the coding matrix a priori, allowing detecting the transmitted QSM bits. Importantly, the proposed scheme has automatic user tracking ability with no CSI needed at the desired receiver and can handle receivers with highly correlated channels due to angular-range focusing profile. Further, secrecy outage probability (SOP), asymptotic lower bound on Eve's detecting error probability, and average data leakage rate are analysed without Eve's CSI. The proposed scheme reveals essential secrecy information that is not captured by the classical SOP and is more power efficient.

The rest of the paper is organized as follows. Section 2 presents the proposed scheme. In Section 3, performance metrics are devised to evaluate the proposed scheme. In Section 4, numerical results are presented, and finally, in Section 5, we draw conclusions.

2. PROPOSED CODING MATRIX FREQUENCY MODULATED DIVERSE RETRODIRECTIVE ARRAY SECURE TRANSMITTER

2.1. System Model

Consider a mmWave communication FMD-RDA transmitter system (see Fig. 1) where the desired transceiver wants to communicate, and a passive Eve tries to intercept the data (see the time frame block in Fig. 2). To establish secure transmission, we make the following assumptions:

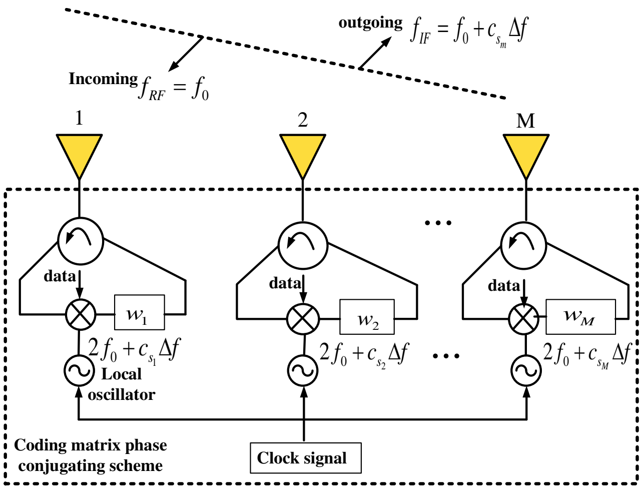

Figure 1. Proposed coding matrix frequency modulated diverse retrodirective array secure transmitter for QSM transmission in mmWave communications: Note $c_{s_m} = \{c_{s_1}, c_{s_2}, \cdots c_{s_M}\}$ denotes the coding matrix for frequency increments Δf, namely $\{1, 2, 4, 8, 5, 10, 9, 7, 3, 6\}$.

(1) The pilot signal is emitted only by the desired receiver with authentication procedure. We omit how to tackle unwanted incoming pilot signals from Eve in this paper as future work.

(2) Multiple-input single-output (MISO) mmWave wireless communications have perfect synchronization between the proposed transmitter and desired receiver.

(3) To facilitate decoding, the desired receiver should know the coding matrix used for frequency increments designed a prior. Note that the coding matrix can be sent to the desired receiver via a low speed forward link [43].

(4) Eve's activity is to intercept retransmission of the confidential useful data meant for the desired receiver during Phase II as depicted in Fig. 2.

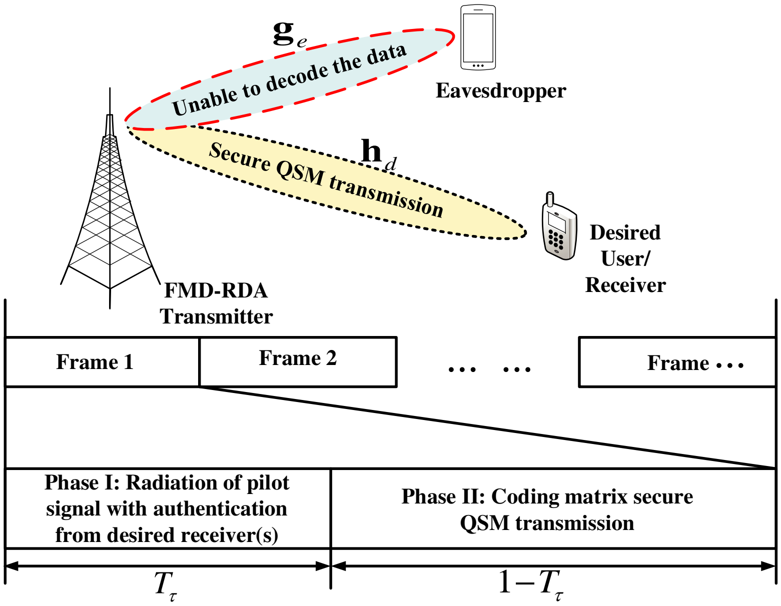
$\mathbf{g}_e$
Unable to decode the data
Eavesdropper
$\mathbf{h}_d$
Secure QSM transmission
Desired User/ Receiver
FMD-RDA Transmitter
Frame 1
Frame 2
… …
Frame …
Phase I: Radiation of pilot signal with authentication from desired receiver(s)
Phase II: Coding matrix secure QSM transmission
T_τ
$1-T_\tau$

Figure 2. Time frame block is decomposed into two phases: The desired receiver emit pilot signal with authentication during T_r in phase I. After the pilot signal, the FMD-RDA transmitter re-transmit the confidential data during $1 - T_r$ in phase II.

2.2. Coding Matrix Design for Secure Transmission

Without loss of generality, we assume coding matrix c_s, i.e., $M = 10$, namely {1, 2, 4, 8, 5, 10, 9, 7, 3, 6} [44, 45] for our analysis, see Fig. 3(a) and Fig. 3(b), for the illustration of the coding matrix and difference matrix. More importantly the utilized order of frequencies (i.e., coding sequence) represents a concise fashion which describes the coding matrix. The difference matrix can be computed by $\Psi_{i,j} = \alpha_{i+j} - \alpha_j$ with $i + j \leq M$. Note that α_i denotes the ith coding element, and $i + j > M$ denote the remaining locations which are left blank. Note that the difference matrix shows that the coding matrix used is feasible. Considering the designed coding matrix, our proposed system allows for ten elements with frequency increments indexed as $c_{s_M}\Delta f$ with $c_{s_M} = \{1, 2, 4, 8, 5, 10, 9, 7, 3, 6\}$, and Δf denotes the frequency hopping step. It is important to note that without specified coding matrix of the frequency increments, it will be difficult to decipher the transmission process.

2.3. QSM Modulator Scheme

Following [32], herein, we demonstrate the principle of QSM transmission. We consider MISO and quadrature amplitude modulation (4-QAM). The bits to be reradiated at a certain time instant are represented by $k = \log_2\left(M_0 M^2\right) = 6\,\text{bits}$. Suppose that $k = \underbrace{[1\ 1\ 0\ 1\ 1\ 1]}_{\log_2(M_0)+\log_2(M^2)}$ are to be emitted to the

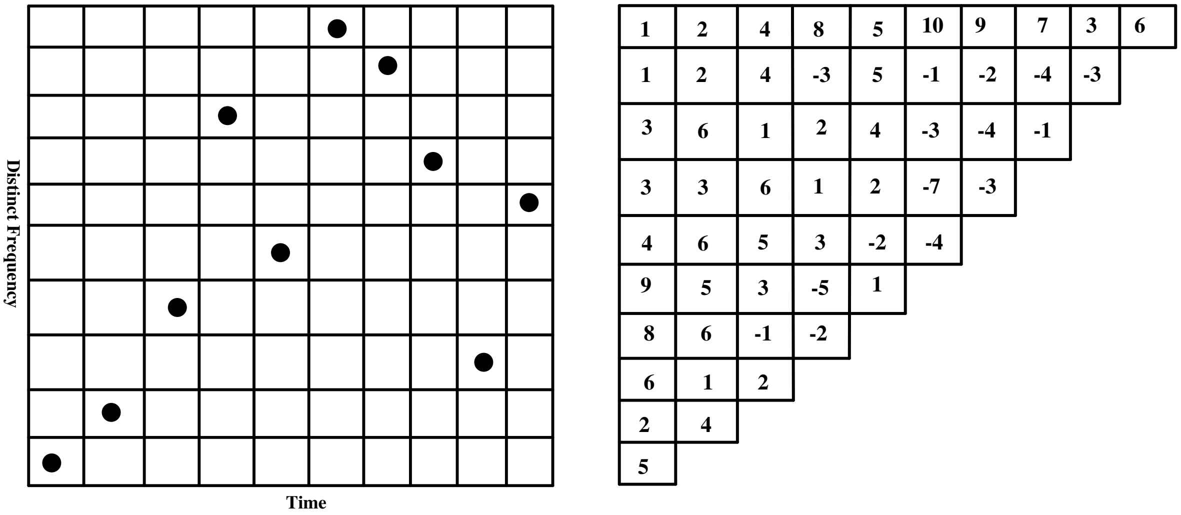

1	2	4	8	5	10	9	7	3	6
1	2	4	-3	5	-1	-2	-4	-3	
3	6	1	2	4	-3	-4	-1		
3	3	6	1	2	-7	-3			
4	6	5	3	-2	-4				
9	5	3	-5	1					
8	6	-1	-2						
6	1	2							
2	4								
5									

(a) (b)

Figure 3. Illustration of (a) Coding matrix c_s, $M = 10$: $\{1, 2, 4, 8, 5, 10, 9, 7, 3, 6\}$ and (b) Difference matrix design.

desired receiver. The first $\log_2(M_0)$ bits [11] modulates the constellation symbol (4-QAM), $x = +1 - j$. This symbol is decomposed into two, namely real part $x_\Re = +1$ and imaginary part $x_\Im = -j$. Next, the $\log_2(M)$ bits, [01], modulate the transmit element i.e., $\ell_\Re = 2$, to emit $x_\Re = +1$. The resultant is a vector $\mathbf{s}_\Re = [0 \ \ +1 \ \ 0 \ \ 0]^T$. Lastly, the $\log_2(M)$ bits, [11], modulate another transmit element, $\ell_\Im = 4$, to radiate $x_\Im = -j$, resulting in the vector $\mathbf{s}_\Im = [0 \ \ 0 \ \ 0 \ \ -j]^T$. The resultant vector is obtained by adding the real and imaginary vectors. Hence, the signal vector to be transmitted is

$$\mathbf{s} = \mathbf{s}_\Re + \mathbf{s}_\Im = [0 \ \ +1 \ \ 0 \ \ -j]^T \tag{1}$$

Vector $\mathbf{s}$ in Eq. (1) is reradiated to the desired receiver by FMD-RDA transmitter over an $(M \times 1)$ mmWave channel $\mathbf{h}_d$. Note that the channel between the FMD-RDA transmitter and Eve is $\mathbf{g}_d$.

2.4. System Formulation

It should be noted that even if beamforming is not formed during retransmission, FMD-RDA is still able to phase conjugate the emitted pilot signal from the desired receiver. As illustrated in Fig. 2, in the first T_τ phase, pilot signal is emitted from the desired receiver (i.e., with authentication) to the FMD-RDA transmitter. Herein, we assume the principle of channel reciprocity. The pilot signal is represented as $s(t) = \exp(2\pi f_0 t)$. The incoming pilot signal is detected at the FMD-RDA transmitter mth element as

$$y_m(t) = \exp\left(j2\pi f_0\left(t - \frac{r' - md\sin\theta_{in}}{c}\right)\right) \tag{2}$$

where the range approximation is ${r'}_m \approx r' - md\sin\theta_{in}$, with r' being range of the desired receiver and FMD-RDA transmitter first reference element. θ_{in} is originated from the desired receiver (i.e., pilot signal incoming angle). According to Fig. 1, the incoming pilot signal received by the FMD-RDA transmitter (i.e., mth element) is mixed with phase-conjugate mixers (i.e., local oscillator (LO) signal), then we have

$$f_{LO}^m = 2f_0 + \Delta f_m(t); \quad m = 1, 2, \ldots, M \tag{3}$$

where $\Delta f_m(t)$ is formulated as

$$\Delta f_m(t) = \sqrt{P_t}\left(h_{\ell_\Re} x_\Re + j h_{\ell_\Im} x_\Im\right) \cdot c_{s_m} \Delta f(t) \tag{4}$$

with Δf smaller than signal frequency f_0. $c_{s_m} = \{c_{s_1}, c_{s_2}, \cdots, c_{s_M}\}$ denotes the coding matrix used to provide LPD during retransmission in phase II; symbols $x_\Re$ and $x_\Im$ represent the QAM modulation constellation; $h_{\ell_\Re}$ and $h_{\ell_\Im}$ are the mmWave channel coefficient between the activated FMD-RDA antennas and desired receiver. $\ell_\Re, \ell_\Im = 1, 2, \cdots M$ and P_t denotes the FMD-RDA transmitted power.

In the second $1 - T_\tau$ phase (see Fig. 2), the retransmitted signal by the FMD-RDA transmitter arriving at a particular time t_1 to the desired receiver is written as

$$\begin{aligned} y\left(t_1; \theta_d = \theta_{in}^d, r_d\right) = & \exp j2\pi f_0 \left(t - \frac{r_d - r'}{c}\right) \sum_{m=1}^{M} w_m \exp j2\pi \Delta f_m \left(t - \frac{r_m}{c}\right) \cdot \\ & \left(t - \frac{r_d - md\sin\theta_d}{c}\right) \exp j2\pi md \frac{\sin\theta_d - \sin\theta_{in}^d}{\lambda} \end{aligned} \tag{5}$$

where w_m is the phase weighting, and λ is the wavelength. Note that noise term is not considered. And $r_m \approx r - md \sin\theta$ has the same physical interpretation as in Eq. (2). It is important to note that the transmitted QSM symbols form part of the retransmit angle-range array factor as seen in Eq. (5).

Similarly, Eve retransmitted signal arriving at a certain time t_2 is also given as

$$\begin{aligned} y\left(t_2; \theta_e = \theta_{in}^e, r_e\right) = & \exp j2\pi f_0 \left(t - \frac{r_e - r'}{c}\right) \sum_{m=1}^{M} w_m \exp j2\pi \Delta f_m \left(t - \frac{r_m}{c}\right) \cdot \\ & \left(t - \frac{r_e - md\sin\theta_e}{c}\right) \exp j2\pi md \frac{\sin\theta_e - \sin\theta_{in}^e}{\lambda} \end{aligned} \tag{6}$$

It should be noted that from Eq. (6), we can deduce that even if Eve receives the retransmitted useful signal from FMD-RDA transmitter, it will still be difficult to decode it without the specified coding matrix used for designing the frequency increments.

Remark: The FMD-RDA transmitter frequency and incident frequency should be equal $f = f_0$. If $f \neq f_0$, according to [46], their frequency differences can be linked directly. Hence, the FMD-RDA transmitter is still feasible to offer security capability.

2.5. Optimal Maximum Likelihood (ML) Detection

Note that since the desired receiver radiates pilot signal to the FMD-RDA transmitter, there is no need of CSI at the receiver. Therefore, using the optimal ML detector, we have

$$\begin{aligned} \left[\hat{\ell}_\Re, \hat{\ell}_\Im, \hat{x}_\Re, \hat{x}_\Im\right] & = \arg \min_{\ell_\Re, \ell_\Im, x_\Re, x_\Im} \left\| y\left(t_1, \theta_d = \theta_{in}^d, r_d\right) - \sqrt{P_t}\left(h_{\ell_\Re} x_\Re + j h_{\ell_\Im} x_\Im\right) \cdot c_{s_m} \Delta f \right\|^2 \\ & = \arg \min_{\ell_\Re, \ell_\Im, x_\Re, x_\Im} \|\Psi\|^2 - 2\Re\left\{ y^H \left(t_1, \theta_d = \theta_{in}^d, r_d\right) \Psi \right\} \end{aligned} \tag{7}$$

where $\Psi = \sqrt{P_t}\left(h_{\ell_\Re} x_\Re + j h_{\ell_\Im} x_\Im\right) \cdot c_{s_m} \Delta f$. In order to retrieve the original useful information bits, the receiver used the detected antenna $\hat{\ell}_\Re$ and $\hat{\ell}_\Im$ along with the detected data symbols, namely $\hat{x}_\Re$ and $\hat{x}_\Im$. In addition, we assume that the receiver knows the coding matrix c_{s_m} used for the frequency increment a prior.

3. PERFORMANCE ANALYSIS

3.1. Secrecy Outage Probability (P_s)

The achievable rate from the FMD-RDA transmitter to the desired receiver is determined by

$$C_d\left(\theta_d, r_d, t\right) = \log_2\left(1 + \gamma_d\left(t\right)\right) \tag{8}$$

where received instantaneous signal-to-noise ratio (SNR) at time t is

$$\gamma_d\left(t\right) = \sigma_d^{-2} \left| \mathbf{w}^H \mathbf{a}\left(\theta_d = \theta_{in}^d, r_d, t + \frac{r_d}{c}\right) \right|^2 \tag{9}$$

with $\mathbf{w}$ denoting the transmitter weight vector, σ_d^2 the desired receiver variance, and r_d/c the signal propagation that will arrived at the desired receiver.

Likewise, the achievable rate from the FMD-RDA transmitter to Eve receiver is

$$C_d\left(\theta_d, r_d, t\right) = \log_2\left(1 + \gamma_d\left(t\right)\right) \tag{10}$$

where

$$\gamma_e\left(t\right) = \sigma_e^{-2}\left|\mathbf{w}^H\mathbf{a}\left(\theta_e = \theta_{in}^e, r_e, t + \frac{r_e}{c}\right)\right|^2 \tag{11}$$

Eq. (11) has the same physical meaning as Eq. (9). The exponential distributions of the desired receiver and Eve are given respectively as

$$f_d\left(\gamma_d\left(t\right)\right) = \frac{1}{\bar{\gamma}_d\left(t\right)}\exp\left(-\frac{\gamma_d\left(t\right)}{\bar{\gamma}_d\left(t\right)}\right) \tag{12}$$

$$f_e\left(\gamma_e\left(t\right)\right) = \frac{1}{\bar{\gamma}_e\left(t\right)}\exp\left(-\frac{\gamma_e\left(t\right)}{\bar{\gamma}_e\left(t\right)}\right) \tag{13}$$

For the sake of simplicity, we define the received average SNRs along the desired receiver and Eve, respectively as $\bar{\gamma}_d\left(t\right) = P_t\sigma_d^{-2}$ and $\bar{\gamma}_e\left(t\right) = P_t\sigma_e^{-2}$.

Now, we consider the wiretap encoding technique [47]. Two rates are chosen by the encoder for the QSM bits, namely, codewords rate R_b and confidential data rate R_s. The rate cost to offer anti-eavesdropping is determined by the rate positive difference $R_e \overset{\Delta}{=} R_b - R_s$. Suppose that we construct k length wiretap code which generates 2^{kR_b} codewords $x^k\left(\ell, \xi\right)$, with $\ell = 1, 2, \ldots, 2^{kR_s}$ and $\xi = 1, 2, \ldots, 2^{k\left(R_b - R_s\right)}$. ξ is selected randomly from $\left\{1, 2, \ldots, 2^{k\left(R_b - R_s\right)}\right\}$ for the message index ℓ, having uniform probability and transmit codeword $x^k\left(\ell, \xi\right)$. In this paper, fixed transmission rate is considered. This implies that R_b and R_s will be fixed over t. The desired receiver can detect the data correctly if $C_d\left(\theta_d, r_d, t\right) > R_b$. If $C_e\left(\theta_e, r_e, t\right) > R_e$ then security is compromised.

Following [48], we analyze the secrecy outage probability P_s as follows: The wiretap code maximum achievable fractional equivocation for the proposed scheme is

$$\Phi = \begin{cases} 1, & \text{if } C_e\left(\theta_e, r_e, t\right) \leq R_b - R_s \\ \left(R_b - C_e\left(\theta_e, r_e, t\right)\right)/R_s, & \text{if } R_b - R_s < C_e\left(\theta_e, r_e, t\right) < R_b \\ 0, & \text{if } R_b \leq C_e\left(\theta_e, r_e, t\right) \end{cases} \tag{14}$$

Therefore, secrecy outage probability P_s is equivalently given by

$$\begin{aligned} P_s =& \mathbb{P}\left(\Phi < \psi\right) \\ =& \mathbb{P}\left(2^{R_b} - 1 \leq \gamma_e\left(t\right)\right) + \mathbb{P}\left(2^{R_b - R_s} - 1 < \gamma_e\left(t\right) < 2^{R_b} - 1\right) \\ & \cdot \mathbb{P}\left(\frac{R_b - C_e\left(\theta_e, r_e, t\right)}{R_s} < \psi \left| 2^{R_b - R_s} - 1 < \gamma_e\left(t\right) < 2^{R_b} - 1\right.\right) \\ =& \exp\left(-\frac{2^{R_b - \psi R_s} - 1}{\bar{\gamma}_e\left(t\right)}\right) \end{aligned} \tag{15}$$

with $0 < \psi \leq 1$ giving the distinct secrecy options of P_s. Note that if $\psi = 1$, then classical SOP is obtained [49] meaning perfect secrecy, but note that we cannot always achieve perfect secrecy.

3.2. Eve's Detecting Error Probability Lower Bound Analysis

The proposed scheme average fractional equivocation is determined as

$$\begin{aligned} \bar{\Phi} &= E\left\{\Phi\right\} \\ &= \int\limits_0^{2^{R_b - R_s} - 1} f_e\left(\gamma_e\left(t\right)\right)d\gamma_e + \int\limits_{2^{R_b - R_s} - 1}^{2^{R_b} - 1}\left(\frac{R_b - C_e\left(\theta_e, r_e, t\right)}{R_s}\right)f_e\left(\gamma_e\left(t\right)\right)d\gamma_e \\ &= 1 - \left(R_s\,\text{In}\left(2\right)\right)^{-1}\exp\left(\bar{\gamma}_e\left(t\right)\right)^{-1}\left(E_i\left(-\frac{2^{R_b}}{\bar{\gamma}_e\left(t\right)}\right) - E_i\left(-\frac{2^{R_b - R_s}}{\bar{\gamma}_e\left(t\right)}\right)\right) \end{aligned} \tag{16}$$

where the exponential integral is denoted as $E_i\left(\kappa\right) = \int\limits_{-\infty}^{\kappa}\exp\left(t\right)/t\;dt$. Explicitly, Eq. (16) highlights the lower bound on Eve's detecting error probability asymptotically.

3.3. Average Data Leakage Rate Analysis

As previously stated, we adopt fixed transmission rate, and therefore, we formulate the average data leakage rate as

$$\begin{aligned} AD_L &= \left(1-\bar{\Phi}\right) R_s \\ &=(\text{In}\,(2))^{-1} \exp\left(\bar{\gamma}_e\,(t)\right)^{-1} \left(E_i\left(-\frac{2^{R_b}}{\bar{\gamma}_e\,(t)}\right) - E_i\left(-\frac{2^{R_b-R_s}}{\bar{\gamma}_e\,(t)}\right)\right) \end{aligned} \tag{17}$$

It is important to note that Eq. (17) reveals averagely how the QSM bits can be leaked to Eve during the transmission process.

4. NUMERICAL RESULTS

Suppose that the desired receiver is located at $(50°, 6\,\text{km})$, and $t_1 = 0.02\,\text{ms}$ indicates the reradiated wave arriving at the desired location. Eve is located at $(30°, 8\,\text{km})$ with $t_2 = 0.0277\,\text{ms}$. The coding matrix for $M = 4$ and 6 are respectively given as $\{1, 2, 4, 3\}$ and $\{1, 3, 2, 6, 4, 5\}$. $f_0 = 30\,\text{GHz}$, $\Delta f = 200\,\text{kHz}$, and $R_b = 1 = R_s$. For the next transmission, pilot signal frequency f_0 needs to be estimated.

As already stated in Subsection 2.2, without the specified coding matrix of the frequency increments, it will be difficult to decipher the transmission process. In Fig. 4, we provide coding matrix FDM-RDA beamforming with $M = 10$. It can be seen from the figure that the beamforming shows random-like distributions without obvious peak. This means that it will be difficult for any unfriendly receiver(s) to detect the peak without the specified coding matrix adopted for the frequency increment. Analogous to this scenario, it is expected that using the coding matrix, it will be difficult for the eavesdropper(s) to decipher it.

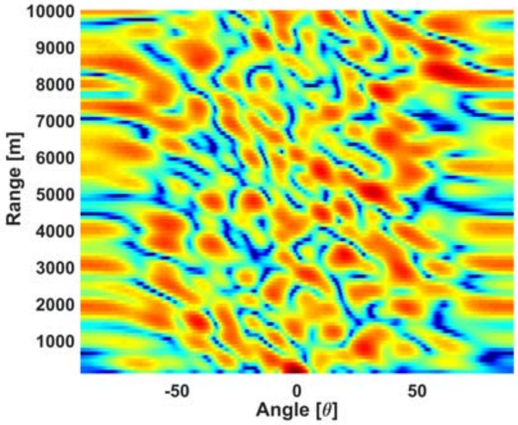

Figure 4. Coding matrix FDM-RDA beamforming with $M = 10$ at desired receiver location $(50°, 6\,\text{km})$.

Figure 5 plots SOP as a function of R_s. It can be noticed that for distinct values of ψ and coding matrix M, we achieve different secrecy performances. It should be mentioned that we can obtain perfect secrecy when $\psi = 1$. Also, it is observed that as SOP increases so does the confidential data rate. This implies that as M increases,the level of system secrecy becomes better.

As depicted in Fig. 6, we plot the average fractional equivocation $\bar{\Phi}$ as a function of $\bar{\gamma}_e\,(t)$ for different values of coding matrix M. From the figure, we notice that $\bar{\Phi}$ decreases as $\bar{\gamma}_e\,(t)$ increases. In essence, Eve may detect useful data when $M \leq 6$.

In Fig. 7, we show the average data leakage rate AD_L against $\bar{\gamma}_e\,(t)$ for different values of coding matrix M. We find that AD_L increases as $\bar{\gamma}_e\,(t)$ increases. This means that the useful data can be leaked to Eve's location with $M \leq 6$.

Note that Fig. 5, Fig. 6 and Fig. 7, reveal three pieces of important secrecy information about the proposed system, namely: (a) distinct secrecy performances leading to perfect secrecy, (b) project the

Eve detectability (i.e., worst scenario), and (c) how likely the useful data can be leaked to Eve. Note that these pieces of information are not captured when using the classical SOP [48].

Finally, Fig. 8 compares the security performance using bit error rate (BER). It can be seen that Eve performs worse (i.e., with no coding matrix a priori) than the desired receiver (i.e., with coding matrix a priori). This implies that the proposed scheme has offered good security transmission.

As shown in Fig. 9, the proposed scheme in MISO setup has better secrecy performance than [30] and [33]. Their secrecy rate values are around 9 bps/Hz, 6.4 bps/Hz and 7.4 bps/Hz, at 30 dB, respectively. In Table 1, we summarize the results of the proposed scheme [30] and [33].

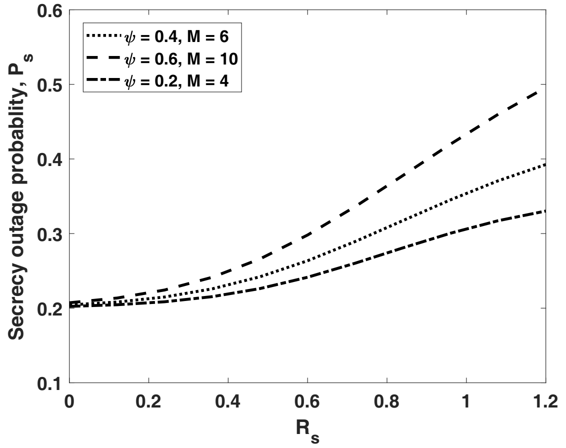

Figure 5. SOP as function of R_s for distinct values of ψ and coding matrix M.

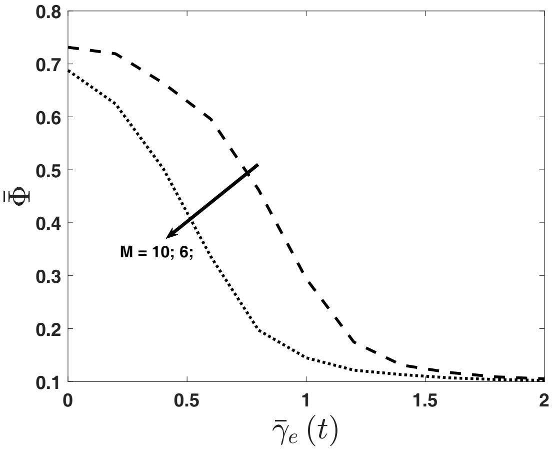

Figure 6. Illustration of $\bar{\Phi}$ as a function of $\bar{\gamma}_e\,(t)$ for distinct values of coding matrix M.

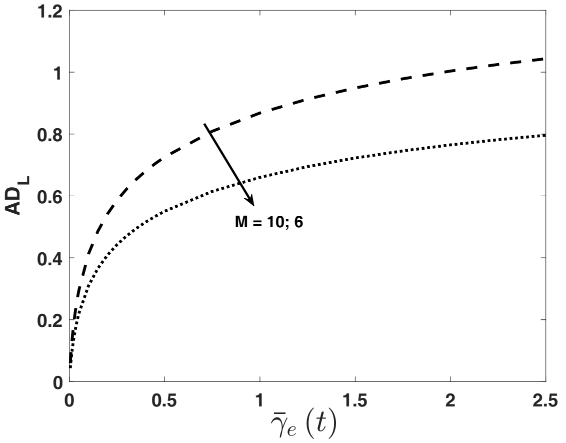

Figure 7. Illustration of AD_L against $\bar{\gamma}_e\,(t)$ for distinct values of coding matrix M.

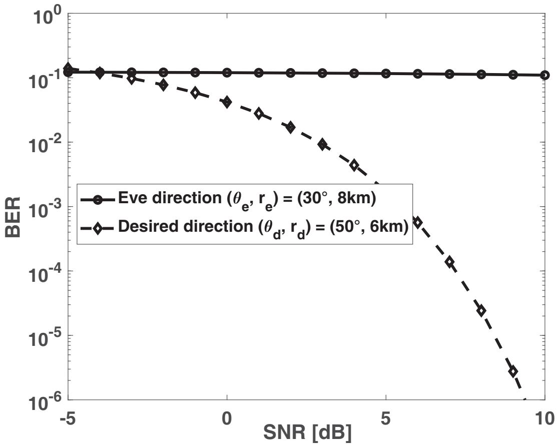

Figure 8. BER comparisons between desired receiver (i.e., at $t_1 = 0.02\,\text{ms}$) and Eve receiver (i.e., at $t_2 = 0.0277\,\text{ms}$).

Table 1. Summary of results.

Parameters	Propose scheme	Ref. [30]	Ref. [33]
Secrecy rate	9 bps/Hz	6.4 bps/Hz	7.4 bps/Hz
Transmit focusing	Range-angle	Only angle	Only angle
CSI requirement	No	Yes	Yes
Automatic user tracking	Yes	No	No

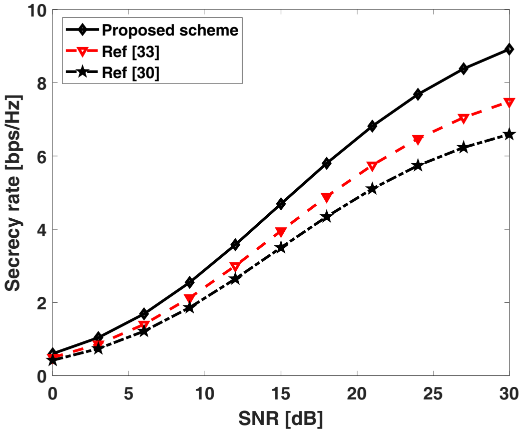

Figure 9. Secrecy rate vs SNR comparisons.

5. CONCLUSION

In this paper, we have proposed an energy efficient security scheme using coding matrix FMD-RDA for QSM transmission in mmWave system. The proposed scheme provides LPD, thus, it is difficult to decipher the coding matrix used. On the other hand, the proposed scheme reveals important secrecy insights which are not captured by classical SOP, namely, different secrecy performance options, Eve's detecting capability, and how fast the useful data are leaked towards Eve location. Our future work will be how to tackle unwanted incoming pilot signals from illegal interrogator (Eve) with new transmission techniques.

REFERENCES

1. Xiao, M., S. Mumtaz, Y. Huang, et al., "Millimeter wave communications for future mobile networks," *IEEE Journal on Selected Areas in Communications*, Vol. 35, No. 9, 1909–1935, Sep. 2017.
2. Niu, Y., Y. Li, D. Jin, et al., "A survey of millimeter wave communications (mmwave) for 5G: opportunities and challenges,“ *Wireless Networks*, Vol. 21, No. 8, 2657–2676, Apr. 2015.
3. Andrews, J. G., T. Bai, M. N. Kulkarni, et al., "Modeling and analyzing millimeter wave cellular systems," *IEEE Transactions on Communications*, Vol. 65, No. 1, 403–430, Jan. 2017.
4. Zhang, J. A., X. J. Huang, V. Dyadyuk, and Y. J. Guo, "Massive hybrid antenna array for millimeter wave cellular communications," *IEEE Wireless Communications*, Vol. 22, No. 1, 79–87, Feb. 2015.
5. Mohammad, A., B. S. Virdee, A. Ali, E. Limiti, "Extended aperture miniature antenna based on CRLH metamaterials for wireless communication systems operating over UHF to C-band," *Radio Science*, Vol. 53, No. 2, 154–165, Feb. 2018.
6. Mohammad, A., B. S. Virdee, P. Shukla, et al., "Interaction between closely packed array antenna elements using meta-surface for applications such as mimo systems and synthetic aperture radars," *Radio Science*, Vol. 53, No. 11, 1368–1381, Nov. 2018.
7. Mohammad, A., B. S. Virdee, C. H. See, et al., "Study on isolation improvement between closely-packed patch antenna arrays based on fractal metamaterial electromagnetic bandgap structures," *IET Microwaves, Antennas and Propagation*, Vol. 12, No. 14, 2241–2247, 28 Nov. 2018.
8. Mohammad, A., B. S. Virdee, P. Shukla, et al., "Meta-surface wall suppression of mutual coupling between microstrip patch antenna arrays for thz-band applications," *Progress In Electromagnetics Research Letters*, Vol. 75, 105–111, 2018.
9. Mohammad, A., M. N. -M. Mohammad, R. A. Sadeghzadeh, et al., "Traveling-wave antenna based on metamaterial transmission line structure for use in multiple wireless communication

applications," *International Journal of Electronics and Communications*, Vol. 70, No. 12, 1645–1650, Dec. 2016.

10. Mohammad, A., M. N.-M. Mohammad, R. A. Sadeghzadeh, et al., "New CRLH-based planar slotted antennas with Helical inductors for wireless communication systems, RF-circuits and microwave devices at UHF-SHF bands," *Wireless Personal Communications*, Vol. 92, No. 3, 1029–1038, Feb. 2017.
11. Mohammad, A., E. Limiti, M. N.-M. Mohammad, et. al., "A new wideband planar antenna with band-notch functionality at GPS, bluetooth and WiFi bands for integration in portable wireless systems," *International Journal of Electronics and Communications*, Vol. 72, 79–85, Feb. 2017.
12. Mohammad, A., B. S. Virdee, A. Ali, and E. Limiti, "Miniaturized planar-patch antenna based on metamaterial L-shaped unit-cells for broadband portable microwave devices and multiband wireless communication systems," *IET Microwaves, Antennas and Propagation*, Vol. 12, No. 7, 1080–1086, 13 Jun. 2018.
13. Massimo, M. D., M. Toshifumi, and M. M. Hanifbhai, "A compact switched-beam planar antenna array for wireless sensors operating at Wi-Fi band," *Progress In Electromagnetics Research C*, Vol. 83, 137–145, 2018.
14. Donelli, M. and P. Febvre, "An inexpensive reconfigurable planar array for Wi-Fi applications," *Progress In Electromagnetics Research C*, Vol. 28, 71–81, 2012.
15. Mesleh, R. Y., H. Haas, S. Sinanovic, et al., "Spatial modulation," *IEEE Transactions Veh. Technol.*, Vol. 57, No. 4, 2228–2241, Jul. 2008.
16. Di Renzo, M., H. Haas, A. Ghrayeb, et al., "Spatial modulation for generalized MIMO: Challenges, opportunities, and implementation," *Proc. IEEE*, Vol. 102, No. 1, 56–103, Jan. 2014.
17. He, L., J. Wang, C. Zhang, and J. Song, "Improving the performance of spatial modulation by phase-only pre-scaling," *Proc. IEEE Int. Conf. Communications (ICC)*, 3210–3215, London, U.K., Jun. 2015.
18. Li, X. and L. Wang, "High rate space-time block coded spatial modulation with cyclic structure," *IEEE Communications Lett.*, Vol. 18, No. 4, 532–535, Apr. 2014.
19. Stavridis, A., S. Sinanovic, M. D. Renzo, and H. Haas, "Transmit precoding for receive spatial modulation using imperfect channel knowledge," *Proc. IEEE 75th Veh. Technol. Conf. (VTC Spring)*, 1–5, Yokohama, Japan, May 2012.
20. Nusenu, S. Y. and W. Q. Wang, "Range-dependent spatial modulation using frequency diverse array for OFDM wireless communications," *IEEE Trans. Veh. Technol.*, Vol. 67, No. 11, 10886–10895, 2018.
21. Hong, Y.-W. P., P.-C. Lan, and C.-C. J. Kuo, "Enhancing physical layer secrecy in multiantenna wireless systems: An overview of signal processing approaches," *IEEE Signal Process. Mag.*, Vol. 30, No. 5, 29–40, Aug. 2013.
22. Zou, Y. and J. Zhu, *Physical Layer Security for Cooperative Relay Networks*, Springer, New Year, NY, USA, 2016.
23. Trappe, W., "The challenges facing physical layer security," *IEEE Commun. Mag.*, Vol. 53, No. 6, 16–20, Jun. 2015.
24. Xiong, Q., Y. Gong, and Y.-C. Liang, "Achieving secrecy capacity of MISO fading wiretap channels with artificial noise," *Proc. IEEE Wireless Commun. Netw. Conf. (WCNC)*, 1–5, Shanghai, China, Apr. 2013.
25. Sun, L., P. Ren, Q. Du, et al., "Security-aware relaying scheme for cooperative networks with untrusted relay nodes," *IEEE Commun. Lett.*, Vol. 19, No. 3, 463–466, Mar. 2015.
26. Guan, X., Y. Cai, and W. Yang, "On the mutual information and precoding for spatial modulation with finite alphabet," *IEEE Wireless Commun. Lett.*, Vol. 2, No. 4, 383–386, Aug. 2013.
27. Yang, L.-L., "Transmitter preprocessing aided spatial modulation for multiple-input multiple-output systems," *Proc. IEEE Veh. Technol. Conf. (VTC-Spring)*, 1–5, Budapest, Hungary, May 2011.
28. Wu, F., R. Zhang, L.-L. Yang, and W. Wang, "Transmitter precoding aided spatial modulation for

secrecy communications," *IEEE Trans. Veh. Technol.*, Vol. 65, No. 1, 467–471, Jan. 2016.

29. Wu, F., L. L. Yang, W. Wang, and Z. Kong, "Secret precoding-aided spatial modulation," *IEEE Commun. Lett.*, Vol. 19, No. 9, 1544–1547, Sep. 2015.
30. Wang, L., S. Bashar, Y. Wei, and R. Li, "Secrecy enhancement analysis against unknown eavesdropping in spatial modulation," *IEEE Commun. Lett.*, Vol. 19, No. 8, 1351–1354, Aug. 2015.
31. Chen, Y., L. Wang, Z. Zhao, et al., "Secure multiuser MIMO downlink transmission via precoding-aided spatial modulation," *IEEE Commun. Lett.*, Vol. 20, No. 6, 1116–1119, Jun. 2016.
32. Mesleh, R., S. S. Ikki, and H. M. Aggoune, "Quadrature spatial modulation," *IEEE Trans. Veh. Technol.*, Vol. 64, No. 6, 2738–2742, Jun. 2015
33. Huang, Z., Z. Gao, and L. Sun, "Anti-eavesdropping scheme based on quadrature spatial modulation," *IEEE Commun. Lett.*, Vol. 21, No. 3, 532–535, Mar. 2017.
34. Ju, Y., H.-M. Wang, T.-X. Zheng, and Q. Yin, "Secure transmissions in millimeter wave systems," *IEEE Transactions on Communications*, Vol. 65, No. 5, 2114–2127, May 2017.
35. Lin, J., Q. Li , J. Yang, et al., "Physical-layer security for proximal legitimate user and eavesdropper: A frequency diverse array beamforming approach," *IEEE Transactions on Information Forensics And Security*, Vol. 13, No. 3, 671–684, Mar. 2018.
36. Fusco, V. and N. Buchanan, "Developments in retrodirective array technology," *IET Microw., Antennas Propag.*, Vol. 7, No. 2, 131–140, May 2013.
37. Ding, Y., V. F. Fusco, "A synthesis-free directional modulation transmitter using retrodirective array," *IEEE Journal of Selected Topics in Signal Processing*, Vol. 11, No. 2, 428–441, Mar. 2017.
38. Yao, A.-M., W. Wu, and D.-G. Fang, "Frequency diverse array phase conjugating retrodirective array with simultaneous range-focusing capability for multi-targets," *Proceedings of the Asia-Pacific Microwave Conference,* Nanjing, China, 1–3, Dec. 2015.
39. Wang, W. Q., "Retrodirective frequency diverse array focusing for wireless information and power transfer," *IEEE Journal on Selected Areas in Communications*, Vol. 37, No. 1, 61–73, 2019.
40. Mesleh, R. and S. Ikki, "On the impact of imperfect channel knowledge on the performance of quadrature spatial modulation," *Proc. IEEE Wireless Communications and Networking Conference (WCNC)*, 534–538, Mar. 2015.
41. Younis, A., R. Mesleh, and H. Haas, "Quadrature spatial modulation performance over Nakagami-m fading channels," *IEEE Trans. on Veh. Tech.*, Vol. 65, No. 12, 10227–10231, Dec. 2016.
42. Afana, A., R. Mesleh, S. Ikki, and I. Atawi, "Performance of quadrature spatial modulation in amplify-and-forward cooperative relaying," *IEEE Commun. Lett.*, Vol. 20, No. 2, 240–243, Feb. 2016.
43. Shu, F., Z. Wang, R. Chen, et al., "Two high-performance schemes of transmit antenna selection for secure spatial modulation," *IEEE Transactions on Vehicular Technology*, Vol. 67, No. 9, 8969–8973, Sep. 2018.
44. Golomb, S. W. and H. Taylor, "Constructions and properties of Costas arrays," *Proceedings of the IEEE*, Vol. 72, No. 9, 1143–1163, Sep. 1984.
45. Levanon, N. and E. Mozeson, *Radar Signals*, John Wiley and Sons, Inc., Hoboken, New Jersey, 2004.
46. Buchanan, N. B., V. F. Fusco, and M. Van Der Vorst, "Phase conjugating circuit with frequency offset beam pointing error correction facility for precision retrodirective antenna applications," *Proceedings of the 41st European Microwave Conference*, 1281–1283, Manchester, UK, Oct. 2011.
47. Wyner, A. D., "The wire-tap channel," *Bell Syst. Tech. J.*, Vol. 54, No. 8, 1355–1387, Oct. 1975.
48. He, B., X. Zhou and A. Lee Swindlehurst, "On secrecy metrics for physical layer security over quasi-static fading channels," *IEEE Transactions On Wireless Communications*, Vol. 15, No. 10, 6913–6924 Oct. 2016.
49. Zhou, X., M. R. McKay, B. Maham, and A. Hjungnes, "Rethinking the secrecy outage formulation: A secure transmission design perspective," *IEEE Commun. Lett.*, Vol. 15, No. 3, 302–304, Mar. 2011.